Ther Adv Respir Dis
2020, Vol. 14: 1–18
DOI: 10.1177/1753466620915156

Combination therapy of gefitinib and miR-30a-5p may overcome acquired drug resistance through regulating the PI3K/AKT pathway in non-small cell lung cancer

Fengfeng Wang*, Fei Meng*, Sze Chuen Cesar Wong, William C.S. Cho, Sijun Yang and Lawrence W.C. Chan

Abstract

Background: Non-small cell lung cancer (NSCLC) patients with an epidermal growth factor receptor (EGFR) mutation often initially respond to EGFR tyrosine kinase inhibitor (EGFR-TKI) treatment but may acquire drug resistance due to multiple factors. MicroRNAs are a class of small noncoding and endogenous RNA molecules that may play a role in overcoming the resistance.

Materials and methods: In this study, we explored and validated, through *in vitro* experiments and *in vivo* models, the ability of a combination treatment of EGFR-TKI, namely gefitinib, and a microRNA mimic, miR-30a-5p, to overcome drug resistance through regulation of the insulin-like growth factor receptor-1 (IGF1R) and hepatocyte growth factor receptor signaling pathways, which all converge on phosphatidylinositol 3 kinase (PI3K), in NSCLC. First, we examined the hypothesized mechanisms of drug resistance in H1650, H1650-acquired gefitinib-resistance (H1650GR), H1975, and H460 cell lines. Next, we investigated a potential combination treatment approach to overcome acquired drug resistance in the H1650GR cell line and an H1650GR cell implanted mouse model.

Results: Dual inhibitors of EGFR and IGF1R significantly lowered the expression levels of phosphorylated protein kinase B (p-AKT) and phosphorylated mitogen-activated protein kinase (p-ERK) compared with the control group in all cell lines. With the ability to repress PI3K expression, miR-30a-5p mimics induced cell apoptosis, and inhibited cell invasion and migration in the treated H1650GR cell line.

Conclusion: Gefitinib, combined with miR-30a-5p mimics, effectively suppressed the growth of H1650GR-induced tumor in xenografts. Hence, a combination therapy of gefitinib and miR-30a-5p may play a critical role in overcoming acquired resistance to EGFR-TKIs.

The reviews of this paper are available via the supplemental material section.

Keywords: combination therapy, drug resistance, epidermal growth factor receptor, gefitinib, miR-30a-5p, non-small cell lung cancer

Received: 21 November 2019; revised manuscript accepted: 28 February 2020.

Correspondence to:
William C.S. Cho
Department of Clinical Oncology, Queen Elizabeth Hospital, Hong Kong, P.R. China
chocs@ha.org.hk

Sijun Yang
ABSL-3 Laboratory at the Center for Animal Experiment and Institute of Animal Model for Human Disease, Wuhan University School of Medicine, Wuhan, P.R. China
sijuny@vt.edu

Lawrence W.C. Chan
Department of Health Technology and Informatics, The Hong Kong Polytechnic University, Y902, 9/F, Lee Shau Kee Building, Kowloon, Hong Kong, P.R. China
wing.chi.chan@polyu.edu.hk

Fengfeng Wang
Fei Meng
Sze Chuen Cesar Wong
Department of Health Technology and Informatics, The Hong Kong Polytechnic University, Hong Kong, P.R. China

*These authors contributed equally.

Introduction

The leading cause of cancer deaths worldwide is lung cancer, of which over 80% of cases are non-small cell lung cancer (NSCLC).[1,2] The 5-year survival of NSCLC is only around 15%, partly due to metastasis and relapse from current treatment methods.[3,4] According to National Comprehensive Cancer Network (NCCN) Guidelines Insights: Non–Small Cell Lung Cancer (Version 1.2020), platinum-based chemotherapy is used as first-line treatment, but with toxicity and/or limited effectiveness.[5] Recently, targeted therapies for NSCLC patients harboring epidermal growth factor receptor (EGFR) mutations have attracted the attention of researchers with their encouraging clinical outcomes.[6,7] Mutations in EGFR, which could lead to

the hyperactivation of the downstream oncogenic pathways related to cell proliferation and survival, were identified in approximately 10–15% of Caucasians and up to 50% of Asians with NSCLC.[7–9] EGFR, a kind of transmembrane glycoprotein with tyrosine kinase activity, is usually auto-phosphorylated to activate downstream molecules, including mitogen-activated protein kinase (MAPK) and phosphatidylinositol 3 kinase (PI3K).[7–11] EGFR tyrosine kinase inhibitors (TKIs), including gefitinib and erlotinib, represent small molecules that bind to the EGFR tyrosine kinase domain and inhibit subsequent phosphorylation and the signal transduction process.[12] However, the drug response is not usually durable due to acquired resistance. Various acquired resistance mechanisms have been investigated, including EGFR T790M secondary mutation, gene amplification of MET and ERBB2, and the transformation to small cell lung cancer.[13] According to NCCN Guidelines Insights: Non–Small Cell Lung Cancer (Version 1.2020), osimertinib is a third-generation EGFR-TKI that is selective for patients with both EGFR-TKI-responsiveness and T790M mutation.[14,15] The secondary mutation in EGFR T790M is one of the possible causes of drug resistance but covers only about half of cases.[16,17] Meanwhile, activation of alternative tyrosine kinase receptors (TKRs), and their downstream molecules shared with EGFR, has been studied to explore alternative novel underlying mechanisms causing drug resistance.[12,18,19]

Compared with a single receptor inhibitor, combined administration of inhibitors of multiple growth factor receptors may overcome drug resistance and inhibit cancer growth and survival pathways more effectively. EGFR can promote tumor cell survival and proliferation by activating multiple downstream signaling pathways concurrently. Other TKRs, such as hepatocyte growth factor receptor (c-MET) and insulin-like growth factor receptor-1 (IGF1R), perform in a similar way as EGFR by influencing the same downstream signaling pathways.[12] The binding of c-Met with its ligand leads to the activation of the PI3K pathway and mitogenesis.[20,21] Signaling transduction through EGFR and c-MET could promote cell survival and proliferation by activating various common downstream signaling pathways, particularly PI3K/AKT/ERK.[22] Researchers found that IGF1R and EGFR share the same downstream pathways, which lead to tumorigenesis and increased cell proliferation, angiogenesis, and metastasis; one such pathway, which plays a central functional role, is the PI3K/AKT signaling pathway.[23] However, the exact mechanisms whereby alternative TKRs lead to drug resistance remain unclear. Thus, identifying the key shared downstream signaling molecules of multiple growth factor receptors may provide useful information for developing therapeutic agents blocking signals from multiple activated growth factor receptors.

MicroRNAs (miRNAs) are short, endogenous, non-coding RNA molecules of 21–25 nucleotides in length that play important roles in altering the expression of target oncogenes or tumor suppressor genes in human cancers.[24–27] MiRNAs are reported to be involved in drug resistance in cancer, and could be regarded as therapeutic targets for lung cancer.[28,29] According to the results of multiple linear regression and support vector regression models in our previous study, there is a negative association between the expression levels of miR-30a-5p and phosphoinositide-3-kinase regulatory subunit 2 (PIK3R2).[19] In another study, we found that overexpression of miR-30a-5p could significantly reduce expression of PIK3R2 to further induce cell apoptosis, as well as inhibiting cell invasion and migration properties, indicating its potential in overcoming acquired resistance to EGFR-TKIs.[18] We hypothesize that concurrent inhibition of EGFR and the alternative TKR, IGF1R, could overcome resistance to EGFR-TKIs. Since miR-30a-5p could inhibit expression of the shared downstream molecule PI3K, the combination treatment of gefitinib and miR-30a-5p may achieve the same effect as dual inhibition to improve drug responsiveness. Effectiveness could be reflected by the expression levels of phosphorylated downstream molecules AKT and ERK. Four cell lines were chosen for *in vitro* analysis. NCI-H1650 is a gefitinib-sensitive cell line. We followed the procedures of Han et al.[30] to induce gefitinib-resistance in H1650 to develop the cell line H1650GR. NCI-H460 and NCI-H1975 are gefitinib-resistant cell lines. NCI-H1975 has a secondary T790M mutation in EGFR. The mouse xenograft model was established to further validate the effects of the combination therapy of gefitinib and miR-30a-5p mimics *in vivo*. Our study was able to identify a potential role for the combination treatment of gefitinib and miRNA in overcoming acquired resistance to EGFR-TKIs, supporting the development of a novel NSCLC treatment.

Materials and methods

Cell culture and reagents

We purchased the cell lines NCI-H1650, NCI-H1975, and NCI-H460 from the Type Culture Collection of the Chinese Academy of Sciences (Shanghai, China). RPMI-1640 supplemented with 10% fetal bovine serum (FBS) was used to grow the cells, which were incubated at 37°C in 5% CO_2. We purchased the EGFR inhibitor gefitinib (#4765) from Cell Signaling Technology, the IGF1R inhibitor NVP-AEW541 (#S1034) from Selleckchem, the radioimmunoprecipitation assay (RIPA) lysis and extraction buffer (#89900) used to lyse cells from ThermoFisher, and MiR-30a-5p mimics (5′-UGUAAACAUCCUCGAC UGGAAG-3′) and the negative control (NC) RNA oligo (5′-UUCUCCGAACGUGUCAC GUTT-3′) from GenePharma. MiR-30a-5p mimics were transfected using lipofectamine 2000 reagent (#12566014), which was purchased from ThermoFisher. We purchased an Annexin V-FITC Apoptosis Detection Kit (#K101-25) from BioVision, and the CytoSelect™ Cell Invasion Assay Kit (#CBA-110) from Cell Biolabs, Inc.

Establishment of the H1650GR cell line

The H1650GR cell line was established by exposing H1650 cells to gefitinib from January to June 2017 with increasing concentrations starting from 0.02 μM. The treatment dose was increased by 25–50%. The treatment was stopped when no significant cell death was observed. From this stepwise treatment, the final concentration of gefitinib required to form the H1650GR cell line, in which the EGFR T790M mutation was not reported in sequencing results, was 20 μM.[30]

Cell cytotoxicity assay

Cell suspensions (100 μl) of H1650, H1650GR, H1975, and H460 were dispensed in 96-well plates with 5000 cells/well, respectively. The cells in the plates were then incubated for 24 h at 37°C in 5% CO_2. Five 10 μl gefitinib solutions of different concentrations (0.5 μM, 1 μM, 10 μM, 20 μM, and 30 μM) were added to the plates. After a 48-h incubation, 10 μl CCK-8 solutions (#CK04, Dojindo, Japan) were added to each well of the plates. The cells in the plates were then incubated for 2 h in the incubator, and absorbance at 450 nm was measured for calculating cell viability.

Western blotting and antibodies

Cells were washed twice in phosphate-buffered saline (PBS) prior to extraction of protein fractions. The cells were scraped from plates using Eppendorf tips. After adding 400 μl RIPA lysis buffer containing 1 mM sodium ortho vanadate and a protease inhibitor cocktail, samples were homogenized on ice and then constant agitation was maintained for 30 min at 4°C. Lysates were obtained after centrifugation at 13,000 rpm (~16,000 × g for 20 min at 4°C). Using bovine serum albumin (BSA) as a standard, protein concentration was measured by Bradford assay (Coomassie Protein Assay, Pierce, Rockford, IL, USA). After loading 30 μg protein/lane on an 8% polyacrylamide gel and subjecting it to electrophoretic separation by sodium dodecyl sulfate-polyacrylamide gel electrophoresis (SDS–PAGE), we transferred the proteins to polyvinylidene difluoride (PVDF) membranes (Immobilon P, Millipore, Billerica, MA, USA) and probed them with specific primary antibodies from Cell Signaling Technology, USA (EGF Receptor (D38B1) XP® Rabbit mAb, #4267, 1:1000; Phospho-EGF Receptor (Tyr1068) (D7A5) XP® Rabbit mAb, #3777, 1:1000; IGF-I Receptor β (D23H3) XP® Rabbit mAb, #9750, 1:1000; Phospho-IGF-I Receptor β (Tyr1135/1136)/Insulin Receptor β (Tyr1150/1151) (19H7) Rabbit mAb, #3024, 1:1000; Met (D1C2) XP® Rabbit mAb #8198, 1:1000; Phospho-Met (Tyr1234/1235) (D26) XP® Rabbit mAb #3077, 1:1000; PI3 Kinase p85 Antibody, #4292, 1:1000; AKT (pan) (C67E7) Rabbit mAb, #4691, 1:1000; Phospho-AKT (Ser473) (D9E) XP® Rabbit mAb, #4060, 1:2000; p44/42 MAPK (Erk1/2) (137F5) Rabbit mAb #4695, 1:2000; Phospho-p44/42 MAPK (Erk1/2) (Thr202/Tyr204) (D13.14.4E) XP® Rabbit mAb #4370, 1:2000; glyceraldehyde 3-phosphate dehydrogenase (GAPDH; D16H11) XP® Rabbit mAb, #5174, 1:2000). We further incubated the proteins with the appropriate horseradish peroxidase (HRP)-conjugated secondary antibodies (Anti-rabbit IgG, HRP-linked Antibody, #7074, 1:3000). A Kodak 4000R Pro camera was used to detect chemiluminescence. Bands resulting from western blotting were quantified by the product, optical density (OD) × band area, with arbitrary units. GAPDH was regarded as an internal control, and was used to normalize all data.

Luciferase reporter assay

The pmirGLO Dual-Luciferase miRNA Target Expression Vector (Promega, Madison, WI, USA)

was used to examine binding of miR-30a-5p to the target genes PIK3R2 and PIK3 catalytic subunit delta (PIK3CD) in the H1650GR cell line. First, the mutant 3′-untranslated region (UTR) of PIK3CD was generated by mutating three nucleotides in the miR-30a-5p recognized PIK3CD 3′-UTR, and the same method was used to generate the mutant 3′-UTR of PIK3R2. After that, wild-type and mutant 3′-UTR sequences of PIK3CD and PI3KR2, including about 200 bp sequence before and after the putative miR-30a-5p binding site, respectively, adding an internal *Not*I restriction site, were designed by our research team. The designed sequences were then synthesized by GenePharma (Shanghai, China). We introduced the synthesized sequence into the above mentioned vector to form the reporter plasmid according to the manufacturer's instructions. The reporter plasmid was then transiently transfected into cells in the presence of either a miR-30a-5p mimic or NC RNA oligo. The cells were harvested and lysed after being cultured for 48 h, and luciferase activity was measured using the Dual-Luciferase Reporter Assay System (Promega, Madison, WI, USA). Renilla-luciferase was applied for normalization.

Dual inhibition of EGFR and IGF1R

With the combined use of gefitinib and AEW541, the inhibitory effect on the signaling pathway was explored in the H1650GR cell line. The concentrations of gefitinib and AEW541 used followed the manufacturer's instructions. The 10 mg gefinitib powder was dissolved in 2.24 ml DMSO to form a 10 mM stock. The 10 mg AEW541 powder was dissolved in 2.2751 ml DMSO to reconstitute a 10 mM stock. The appropriate stocks were diluted individually to concentrations of 2 μM in culture medium of 10% FBS. The H1650GR cells were seeded in 6-well plates, where 70–80% confluency was achieved in each well after a 24-h incubation; the spent medium was then aspirated. The cells were treated individually for 6 h with three prepared 2-ml samples of media containing gefitinib, AEW541, or a combination of gefitinib and AEW541. Western blot assay was used to quantify expression levels of phosphorylated and total signaling proteins.

Transfection with MiR-30a-5p mimics

The H1650GR cells were seeded on 6-well plates with glass-bottom dishes, where 70–80% confluency was achieved in each well after a 24-h incubation. Lipofectamine 2000 transfection reagent (5 μl) was dissolved in 125 μl of Opti-MEM® I Reduced Serum Medium. MiR-30a-5p mimics (75 pmol) in 125 μl of the same medium were mixed with the transfection reagent and allowed to stand at room temperature for 20 min according to the manufacturer's instructions. The resulting 250 μl transfection solutions were added to each well in 1.75 ml medium. After 6 h, 2 ml fresh medium supplemented with 10% FBS was used to replace the cultures. Cells were then incubated for 24 h. The blank control group received Lipofectamine 2000 reagent only, and the NC group was formed by adding the RNA oligo to the lipofectamine 2000 agent. The resulting samples were used for western blotting, cell apoptosis, invasion, and wound healing assays.

Cell apoptosis assay

The Annexin V-FITC Apoptosis Detection Kit was used to perform the cell apoptosis assay according to the manufacturer's instructions. Cells in the resulting sample were washed twice in PBS in glass-bottom dishes, and 500 μl 1X binding buffer was added. After that, 5 μl of Annexin V-FITC and 5 μl of propidium iodide were added to the cells, which were then incubated for 5 min in the dark at room temperature. Images were taken under a microscope to measure apoptosis signals at 6 h and 12 h after adding Annexin V-FITC. Green staining was seen in the plasma membrane when cells bound to Annexin V-FITC. Red staining throughout the nucleus and green staining on the cell surface were seen in cells having lost membrane integrity. In three individual fields per dish, a 40X objective was used to count apoptotic and total cells for each biological repeat. The cell apoptosis rate was estimated using the formula: percentage apoptosis rate = apoptotic cell number / total cell number x100.

Cell invasion assay

The CytoSelect™ Cell Invasion Assay Kit was used to perform the cell invasion assay according to the manufacturer's instructions. First, 500 μl medium with 10% FBS was added to the lower well of the invasion plate. From cell suspension samples with a concentration of 1.0×10^6 cells/ml in serum-free medium, 300 μl of cell suspension solution was added to the upper chamber of the

kit. Cells were then incubated at 37°C in 5% CO_2 for 24 h. Invasive cells migrated through the basement membrane layer of the kit and adhered to the bottom of the insert membrane. Non-invasive cells remained in the upper chamber. After the process, non-invasive cells were removed carefully. Invasive cells were transferred to a clean well containing 400 µl Cell Stain Solution and incubated for 10 min at room temperature. Microscopic images of the invasive cells were then captured. The stained cells were washed gently in 200 µl Extraction Solution and incubated for 10 min. 100 µl of the resulting solution was transferred to a 96-well microtiter plate and measured the OD at 560 nm using a plate reader.

Wound healing assay

The wound healing assay was used to assess cell migration ability. A straight scratch was made gently in monolayers of cells in 6-well plates using an Eppendorf tip. PBS buffer was then used to wash away the detached cells and serum-free culture medium was added. We took images of cells migrating to the scratch at 0 h, 12 h and 24 h after applying the wound under a microscope. The migration rate was estimated according to the formula: percentage wound healing = [(wound length at 0 h) – (wound length at 12 h or 24 h)] / (wound length at 0 h) × 100.[31]

Animal studies

Athymic BALB/c nude mice (4 weeks old, female, 18–22 g body weight for each mouse) were obtained from the Chinese University of Hong Kong and assigned randomly to five groups (four mice per group): i) H1650 group, H1650 cells were injected and no treatment was given; ii) H1650GR group, H1650GR cells were injected and no treatment was given; iii) H1650 gefitinib+NC group, H1650 cells were injected and treated with gefitinib and NC of microRNA; iv) H1650GR gefitinib+NC group, H1650GR cells were injected and treated with gefitinib and NC; and vi) H1650GR gefitinib+miR-30a-5p group, H1650GR were injected and treated with gefitinib and miR-30a-5p mimics. A flow chart illustrating the design of the animal study is shown in Figure S1.

Mice were anesthetized using a mixture (0.1 ml mixture per 10g body weight) of ketamine (10 mg/ml) and xylazine (1.6 mg/ml). According to the groupings, suspensions of 1×10^6 H1650 or H1650GR cells (in 0.2 ml of PBS) were injected subcutaneously in the lower-right flank of the mice. Four mice were placed in each housing cage with free access to water and food. The housing cages were then transferred to Centralized Animal Facilities of Hong Kong Polytechnic University for further husbandry. The mice were raised in a pathogen-free barrier environment. The mice were monitored for body weight and general condition every day. The size of the xenograft tumor was measured twice per week using calipers, and the volume calculated using the formula: volume = 1/2 (length × width^2). On the 7th day postinoculation, xenografts were established successfully in the mice (mean tumor volume per group was 130–160 mm^3).

Gefitinib was administered at 150 mg/kg/day by oral gavage. According to the grouping, a mixture of 10 µl miR-30a-5p mimics or NC RNA oligo (20 µM) and 10 µl lipofectamine 2000 was injected to the xenograft tumors in a multi-site subcutaneous injection manner at 2-day intervals, and the tumor size was measured simultaneously. After 3 weeks of treatment, the mice were sacrificed and tumor tissues were collected with 4% formalin fixation to prepare paraffin-embedded sections for the immunohistochemistry (IHC) assay. An overdose of anesthetics with combination treatment of ketamine and xylazine was used for euthanasia. The mean tumor size was calculated to evaluate the effects of combination treatment of gefitinib and miR-30a-5p in mice. All measurements were taken by research staff blind to the grouping of the mice.

All experimental procedures were carried out according to the guidelines and protocols approved by the Animal Subjects Ethics Subcommittee of the Hong Kong Polytechnic University (Approval number: 14-15/09-HTI-R-HMRF). A "License to Conduct Experiments" was granted by Department of Health, Hong Kong Government [(14-180) in DH/HA&P/8/2/4 Pt.9].

Immunohistochemistry assay

H1650GR xenograft tumors were collected and fixed in 4% formalin. After paraffin-embedding and slicing, a heat-mediated antigen retrieval process lasting 20 min and using sodium citrate buffer was conducted (#ab64236, Abcam,

Eugene, OR, USA), followed by Tris-buffered saline (TBS) containing 1% Tween (TBST) rinsing for 5 min. The tissue sections were then incubated with endogenous peroxidase blocker for 10 min, and washed twice in TBST. After that, the tissue sections were incubated with primary antibodies against PI3K (#ab86714, Abcam) and p-AKT (#4060, Cell Signaling Technology, Danvers, MA, USA) for 60 min at room temperature, and washed twice in TBST. The HRP-conjugated compact polymer system (#ab64264, Abcam) was used as the secondary antibody for visualization, and staining was detected using diaminobenzidine (DAB). Tissue sections were then counterstained with hematoxylin followed by washing three times in TBST. The IHC score of PI3K and p-AKT was calculated based on the following formula: score = 0×[% cells with no staining(0)] + 1×[% cells staining faint to barely visible (1+)] + 2×[% cells staining weak to moderately (2+)] + 3×[% cells staining strongly (3+)].[32] The products of the quantity and intensity scores were calculated: a final score of 0–1 indicated negative expression (–); 2–3 indicated weak expression (+); 4–5 indicated moderate expression (++); and 6 indicated strong expression (+++). Each sample was tested separately and scored by two pathologists. Divergent scores were discussed until agreement was reached.[32]

Statistical analysis

Based on the results of invasion assay on cell cultures, ODs reflecting invasive cell numbers were 1.2 and 0.9, with standard deviation 0.1 for the miR-30a-5p-transfected cell culture and NC, respectively. The error probability α was 0.05 based on Bonferroni correction, and the power (1–β error probability) is 0.80. The power analysis indicates that the minimum number of mice required for each group is four.

IBM SPSS Statistics 24.0 software was used to perform the statistical analysis. All descriptive statistical values are shown as mean ± standard error of mean (SEM). One-way analysis of variance (ANOVA) followed by Tukey's *post hoc* test allowed multiple and pairwise comparisons of western blotting results. Student's *t* test was applied to determine the statistical significance in the cell apoptosis, invasion and wound healing assays, and animal experiments. Significant differences were defined by *p*-values < 0.05.

Results

Detection of gefitinib resistance levels in H1650, H1650GR, H1975, and H460 cell lines

To investigate the resistance levels of the four cell lines to gefitinib, cytotoxicity assays were performed in H1650, H1650GR, H1975, and H460 cells. After measuring absorbance at 450 nm, cell viability and IC_{50} were calculated (Figure S2). The results demonstrated that IC_{50} values in the three gefitinib-resistant cell lines, H1650GR (IC_{50}: 24.4), H1975 (IC_{50}: 10.2), and H460 (IC_{50}: 13.4), were higher than in the gefitinib-sensitive cell line H1650 (IC_{50}: 8.7). Notably, the H1650GR cell line had the largest IC_{50} value, indicating that this cell line was more resistant to gefitinib compared with the other three cell lines.

Exploration of activation status of the IGF1R and MET pathways in H1650, H1650GR, H1975, and H460 cell lines

Different concentrations of gefitinib (0, 0.1, 1, and 10 μM) were used to treat the H1650, H1650GR, H1975, and H460 cell lines. In order to study activation of downstream molecules, we also tested the expression levels of phosphorylated proteins after treatment.

In the H1650 cell line, the expression levels of phosphorylated EGFR (p-EGFR) and downstream molecules p-AKT and p-ERK decreased with increasing concentration of gefitinib from 0 to 10 μM (Figure 1A), indicating that the high concentration of gefitinib may inactivate signal transduction in the EGFR signaling pathway. However, expression levels of p-IGF1R and p-MET were nearly undetectable in all four experimental groups (Figure 1A), indicating that the IGF1R and MET pathways were not activated, regardless of gefitinib concentration used.

After gefitinib-resistance was induced in the H1650 cell line to form the H1650GR cell line, expression levels of p-EGFR and p-ERK decreased with increasing concentration of gefitinib, whereas there was no obvious decrease in the expression level of p-AKT (Figure 1B), indicating that high concentrations of gefitinib could effectively inhibit phosphorylation of EGFR, but not downstream signal transduction in the EGFR signaling pathway. At all four concentrations of gefitinib, expression of p-IGF1R, but not p-MET, was detected (Figure 1B), indicating that the

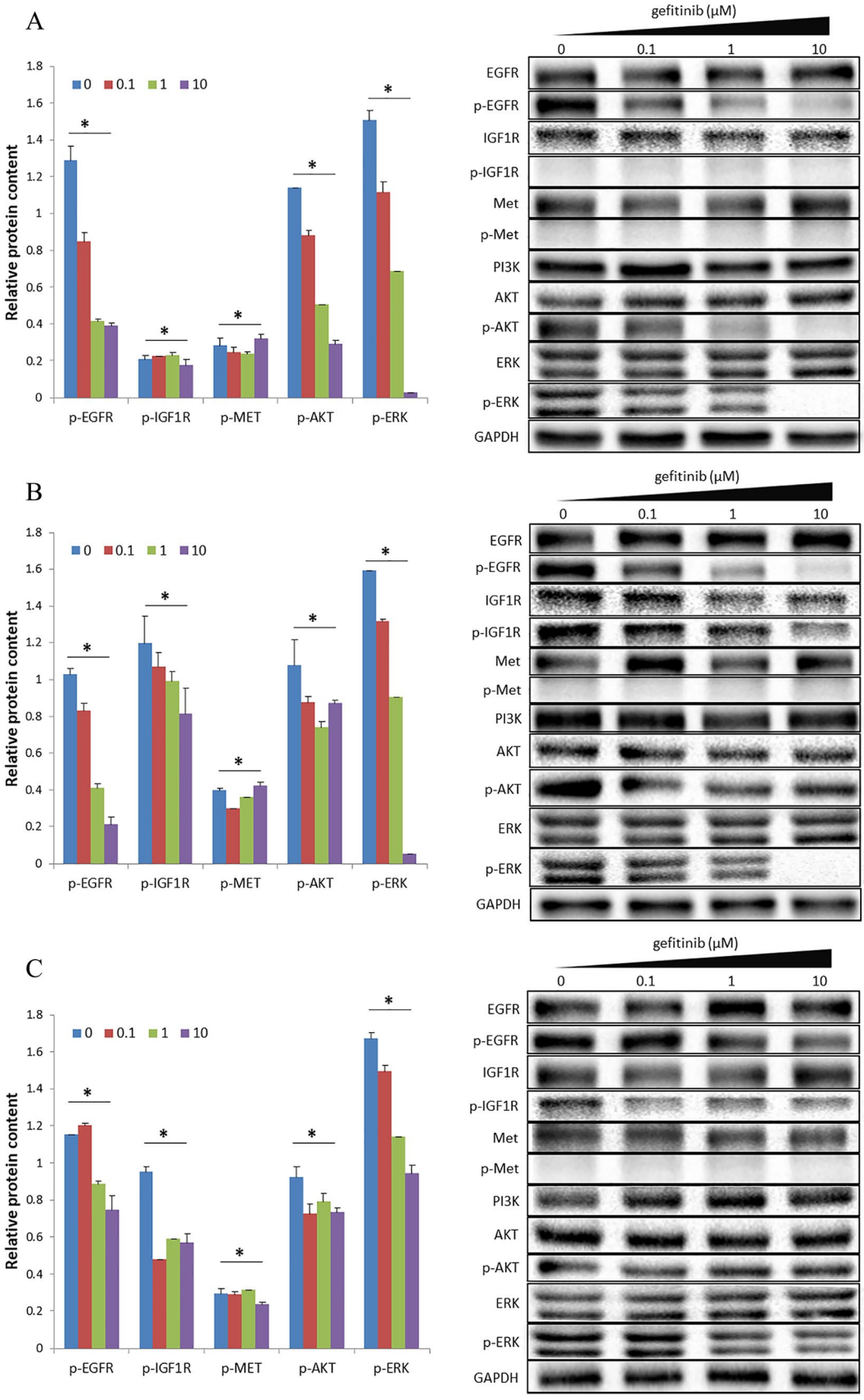

Figure 1. (Continued)

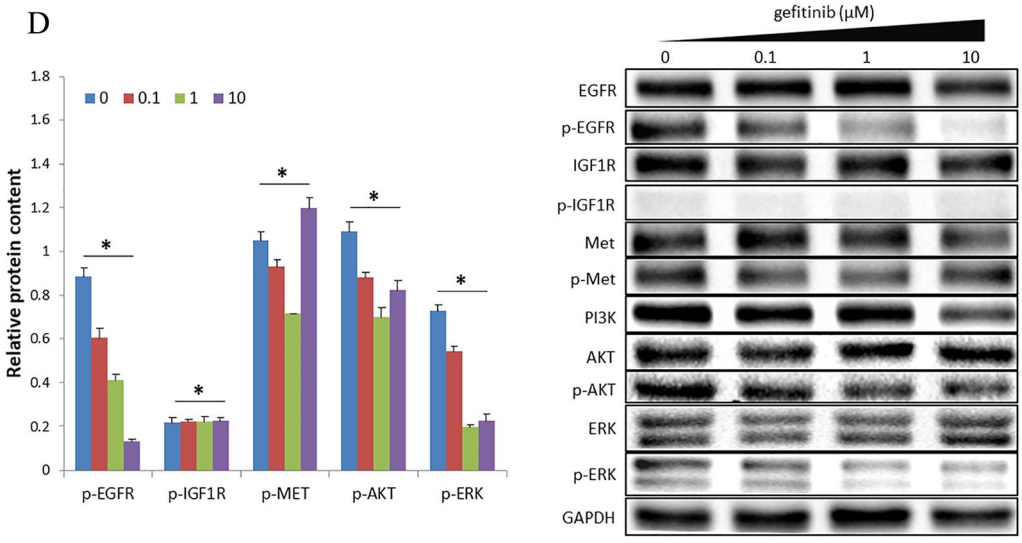

Figure 1. Activation status of IGF1R and MET signaling pathways in terms of protein expression in four cell lines: (A) H1650, (B) H1650GR, (C) H1975, and (D) H460. The internal control was GAPDH. The bar chart presents results as the mean of three independent experiments. Blots are representative of three independent experiments.
*p-value < 0.05. One-way ANOVA was used to compare the four groups with concentrations of gefitinib from 0 to 10 μM.
GAPDH, glyceraldehyde 3-phosphate dehydrogenase; IGF1R, insulin-like growth factor receptor-1; MET, hepatocyte growth factor receptor.

IGF1R pathway was activated, whereas the MET pathway was not.

In the H1975 cell line, there was no obvious decrease in expression levels of p-EGFR and the downstream molecules p-AKT and p-ERK with increasing concentrations of gefitinib (Figure 1C). At all four concentrations of gefitinib tested, expression of p-IGF1R, but not p-MET, was detected (Figure 1C). The results demonstrate that the IGF1R pathway was activated, whereas the MET pathway was not. It is known that a secondary T790M mutation exists in EGFR, whereas the activated IGF1R pathway may be a new mechanism leading to drug resistance in the H1975 cell line.

In the H460 cell line, with increasing concentrations of gefitinib, expression levels of p-EGFR and p-ERK decreased, but p-ERK still exhibited a small amount of expression in the presence of 10 μM gefitinib. Notably, there was no obvious decrease in the expression level of p-AKT (Figure 1D), indicating that high concentrations of gefitinib could effectively inhibit phosphorylation of EGFR, but not inhibit downstream signal transduction in the EGFR signaling pathway. In all four groups, nearly no expression of p-IGF1R was detected. Expression of p-MET was detected, but with no obvious decrease (Figure 1D), indicating that the MET pathway was activated, whereas the IGF1R pathway was not. All results are summarized in Table S1.

Dual inhibition of EGFR and IGF1R blocks shared downstream signaling pathways

Gefitinib, AEW541, or a combination of gefitinib and AEW541 inhibitors were used to treat H1650GR cells. The results revealed significant differences in the expression levels of p-EGFR, p-IGF1R, p-AKT, and p-ERK among the three experimental groups and one control group, with p-values < 0.05 (Figure 2). Compared with gefitinib treatment, AEW541 treatment and the control groups, the combination treatment of gefitinib and AEW541 suppressed p-AKT expression significantly, according to Tukey's *post hoc* test (p-values < 0.05). Hence, the combination treatment could block downstream signaling pathways. The same results were also found in H1975 and H460 cell lines in our previous study.[18] AKT is the downstream molecule in the signaling pathways, and expression levels of the phosphorylated form of AKT were lowest in the dual-inhibitor group, compared with the other three groups.

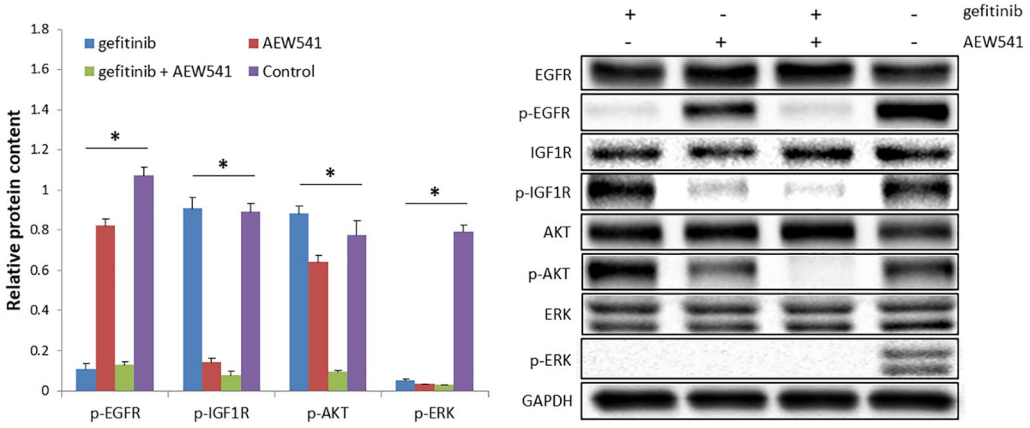

Figure 2. Protein expression in H1650GR cell line subject to EGFR inhibitor (gefitinib), IGF1R inhibitor (AEW541), and dual inhibition (gefitinib+AEW541). The concentration of gefitinib and AEW541 was 2 μM. The internal control was GAPDH. The bar chart shows the results as the mean of three independent experiments. The blots shown are representative images from three independent experiments.
*p-value < 0.05, one-way ANOVA.
ANOVA, analysis of variance; EGFR, epidermal growth factor receptor; GAPDH, glyceraldehyde 3-phosphate dehydrogenase; IGF1R, insulin-like growth factor receptor-1.

Therefore, the PI3K/AKT signaling pathway could be blocked by the dual inhibition of EGFR and IGF1R.

MiR-30a-5p could bind to target genes PIK3R2 and PIK3CD to downregulate expression levels

In our previous studies, miR-30a-5p was found to inhibit expression of PI3K.[18,19] PIK3R2 and PIK3CD are two subunits of PI3K. In this study, the Dual-Luciferase Reporter Assay was used to test the specific binding sites. Wild-type (WT) or mutant (Mut) 3′-UTRs with a dual-luciferase reporter vector were generated (Figure 3A). The results revealed that luciferase activity was significantly decreased in the PIK3R2-WT plasmid with miR-30a-5p mimics compared with PIK3R2-WT plasmid with the NC (p-value < 0.05). However, no significant difference was found between PIK3R2-MUT plasmid with miR-30a-5p mimics compared with PIK3R2-MUT plasmid with the NC (p-value > 0.05) (Figure 3B). The same situation was found for PIK2CD (Figure 3B). Western blotting results showed that overexpression of miR-30a-5p mimics decreased protein levels of PIK3R2 and PIK3CD compared with control groups (Figure 3C). The Dual-Luciferase Reporter Assay and western blotting confirmed association of miR-30a-5p with expression levels of target genes PIK3R2 and PIK3CD in the H1650GR cell line.

Treatment with miR-30a-5p mimics induces cell apoptosis, and inhibits cell invasion and migration

We further explored the effects of miR-30a-5p on cell apoptosis, invasion, and cell migration properties. The cell apoptosis assay demonstrated the effect of miR-30a-5p mimics treatment on apoptosis in the cell line H1650GR. Apoptosis signals were detected, and images were taken at 6 h and 12 h after adding Annexin V-FITC. We then calculated the cell apoptosis rate. In H1650GR cells transfected with miR-30a-5p mimics, the cell apoptosis rate increased significantly at both 6 h and 12 h compared with the NC group (p-values < 0.05) (Figure 4A). The invasion and migration properties were also tested after transfection of miR-30a-5p mimics. Invasion images were recorded, and invasion ability evaluated according to the OD value at 560nm. In H1650GR, the invasive cells of the miR-30a-5p mimic-transfected group were decreased significantly compared with those of the NC group (Figure 4B). Furthermore, cell migration was detected and imaged at 0 h, 12 h, and 24 h after wounding. The results showed that the cell migration rate decreased significantly at both 12 h and 24 h following treatment with miR-30a-5p mimics, compared with the NC group (p-values < 0.05) (Figure 4C). The same results for cell apoptosis, invasion, and migration were also found in both H460 and H1975 cells in our previous study.[18]

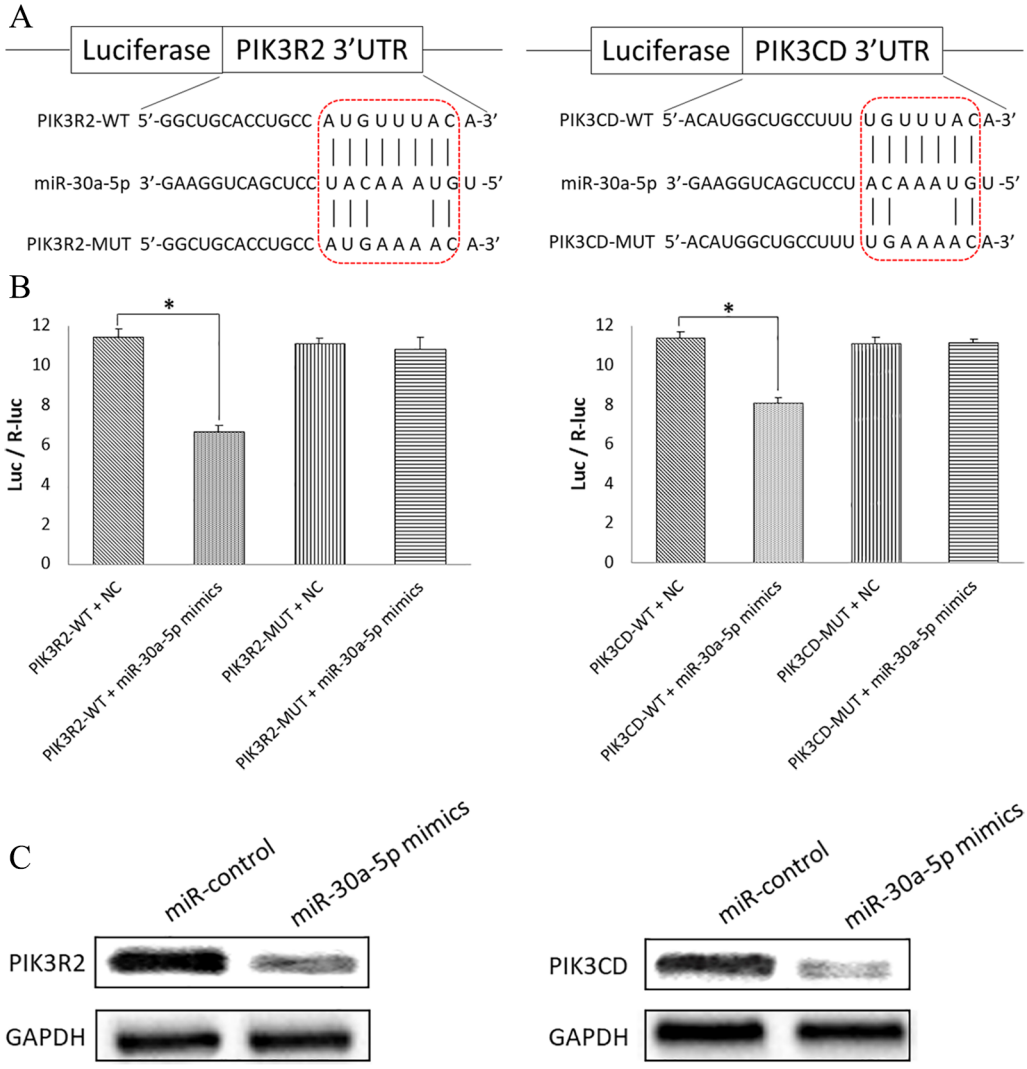

Figure 3. Dual-Luciferase Reporter Assay and western blotting to test binding of miR-30a-5p to, and downregulation of, target genes PIK3R2 and PIK3CD in the H1650GR cell line. (A) Putative miR-30a-5p binding sites in the 3′-UTRs of PIK3R2 and PIK3CD. A mutation was introduced into the 3′-UTR by altering 3 nt in the binding sites, and WT or Mut 3′-UTRs were subcloned into a dual-luciferase reporter vector. (B) Luciferase activities indicating binding between miR-30a-5p and PIK3R2/PIK3CD. Luc/R-luc is the ratio of firefly luciferase to Renilla-luciferase activities. *p-value < 0.05. (C) Western blotting was used to determine the PIK3R2 and PIK3CD protein expression levels in cells transfected with the miR-control or miR-30a-5p mimics. The internal control was GAPDH.
GAPDH, glyceraldehyde 3-phosphate dehydrogenase; PIK3CD, phosphatidylinositol 3 kinase catalytic subunit delta; PI3KR2, phosphatidylinositol 3 kinase regulatory subunit 2; UTR, untranslated region; WT, wild type.

Combination treatment with gefitinib and miR-30a-5p mimics decreases expression levels of p-AKT and p-ERK in the H1650GR cell line

We then explored the effects of combination treatment with gefitinib and miR-30a-5p on downstream molecules in the signaling pathway. H1650GR cells were further transfected with MiR-30a-5p mimics, and gefitinib was added to the culture medium. Protein expression levels were then measured in the four groups: miR-30a-5p mimics, gefitinib+miR-30a-5p mimics, gefitinib+NC, and NC groups. p-AKT expression levels were decreased significantly in the miR-30a-5p mimics group, the gefitinib+miR-30a-5p mimics group and the gefitinib+NC group, compared with the NC group, according to Tukey's *post hoc* test (p-values < 0.05) (Figure 5). The expression levels of p-ERK were decreased significantly in

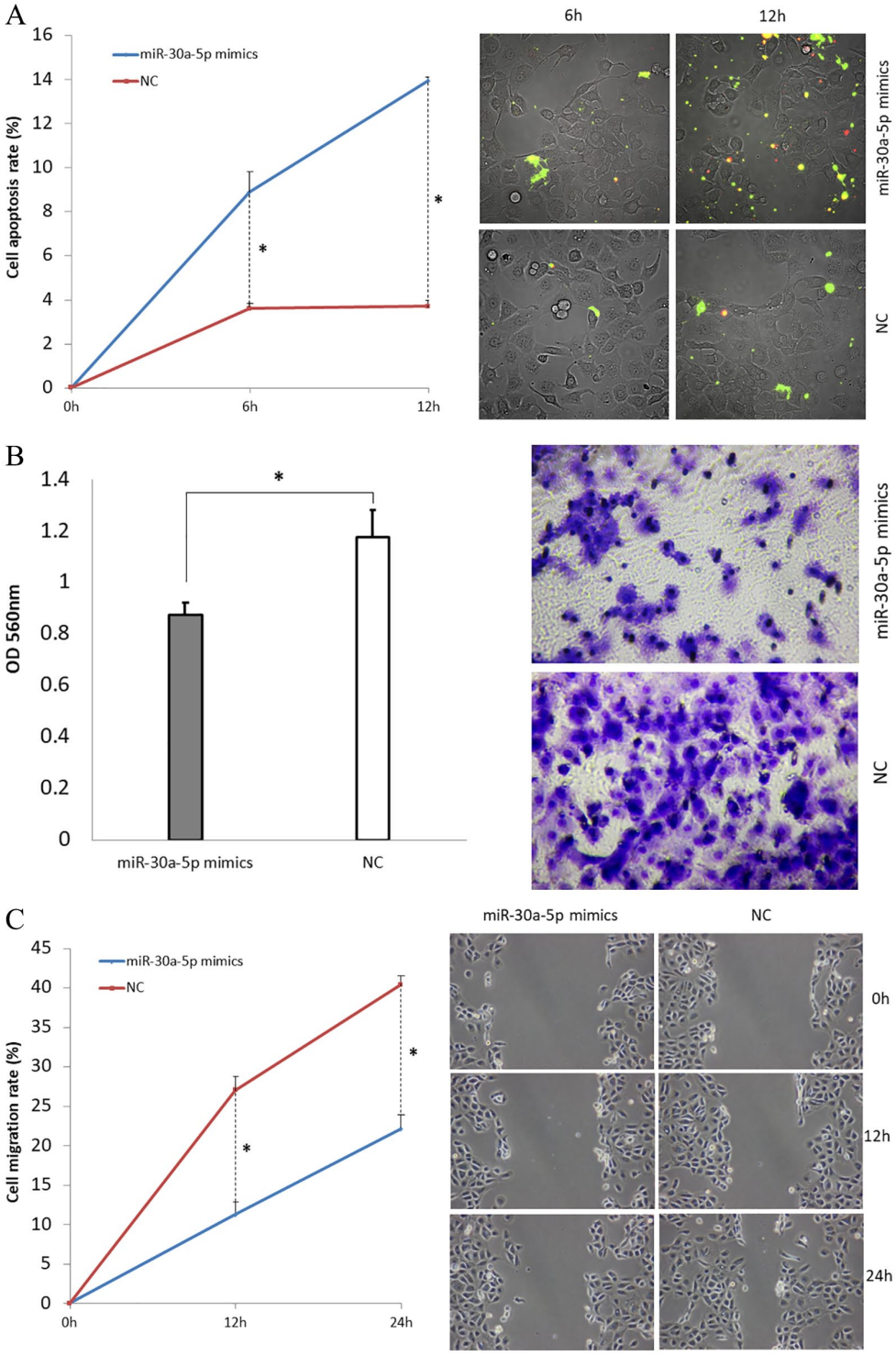

Figure 4. H1650GR cell line assays following transfection with miR-30a-5p mimics. (A) Cell apoptosis assay. The chart shows the results as the mean of three independent experiments. Green represents the early stage of cell apoptosis, and red represents apoptotic cells at the late stage. (B) Cell invasion assay. Invasive cells at the bottom of the invasion membrane were stained and quantified by measuring OD at 560nm after extraction. The bar chart presents the results as the mean of three independent experiments. *p-value < 0.05. (C) Cell wound healing assay. At 0 h, 12 h, and 24 h after the wound was induced, microscopy images of cells migrating towards the scratch were taken. The chart presents the results as the mean of three independent experiments. Wound length was measured to calculate migration rate. Representative microscopy images are shown.
OD, optical density.

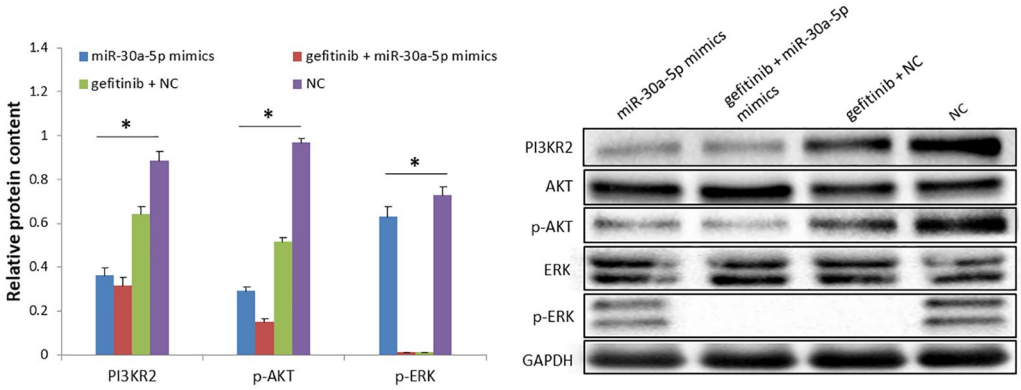

Figure 5. Combination treatment effect of gefitinib and miR-30a-5p mimics on the expression levels of p-AKT and p-ERK in the H1650GR cell line. The bar chart presents results as the mean of three independent experiments. Blots shown are representative of three independent experiments.
*p-value < 0.05, one-way ANOVA.
ANOVA, analysis of variance.

both the gefitinib+miR-30a-5p mimics and gefitinib+NC groups, compared with the NC group (p-values < 0.05). The expression levels of p-AKT and p-ERK were lowest in the combination treatment group compared with the other three groups. In conclusion, the combination treatment of gefitinib+miR-30a-5p mimics significantly decreased expression of p-AKT and p-ERK.

The combination treatment of gefitinib and miR-30a-5p inhibits H1650GR induced xenograft tumor growth in vivo

No adverse events were found in the experiment. The mean tumor volumes of the H1650, H1650GR, H1650 gefitinib+NC, H1650GR gefitinib+NC, and H1650GR gefitinib+miR-30a-5p groups in the first 19 days after the xenograft models were established are shown in Figure 6A. After a 3-week treatment, the mice were sacrificed and the collected tumors are shown in Figure 6B. From the first to the last day of the observation period, the tumor size in the H1650GR group was always significantly larger than that in the H1650 group. Following gefitinib treatment, the tumor size of the H1650 gefitinib+NC group was larger than that of the H1650 group, but the difference was not significant (p-values > 0.05). There was also no significant difference between the H1650GR group and the H1650GR gefitinib+NC group (p-values > 0.05). Starting from the 3rd day, the tumor size of the H1650GR gefitinib+miR-30a-5p group was significantly lower than that of the H1650GR gefitinib+NC group according to Tukey's *post hoc* test (p-values < 0.05). No significant difference was found between the H1650GR gefitinib+miR-30a-5p group and the H1650 gefitinib+NC group throughout the observation period (p-values > 0.05). On the 19th day, the H1650GR gefitinib+miR-30a-5p group not only formed substantially smaller tumors ($508 \pm 74\,mm^3$) than the H1650GR gefitinib+NC group ($1558 \pm 206\,mm^3$), but tumor size was also similar to that of the H1650 gefitinib+NC group ($462 \pm 71\,mm^3$). Hierarchical clustering for the mean tumor volume from the five groups was further drawn, indicating two clusters: the H1650GRand H1650GR gefitinib+NC groups, and the H1650 gefitinib+NC and H1650GR gefitinib+miR-30a-5p groups (Figure 6C).

The combination treatment of gefitinib and miR-30a-5p inhibits PI3K/AKT signaling pathway in xenograft tumors in vivo

After a 3-week treatment, the xenograft tumors were collected and sliced for immunohistochemical staining analysis. The results revealed that expression of PIK3R2, the target of miR-30a-5p, was significantly lower in the H1650GR gefitinib+miR-30a-5p group (++) compared with the H1650GR gefitinib+NC group (+++) (p-value < 0.05) (Figure 7). Meanwhile, the expression level of the activated AKT (p-AKT), a downstream molecule of the PI3K/AKT pathway, was also significantly reduced in the H1650GR gefitinib+miR-30a-5p group (++) compared with the H1650GR gefitinib+NC group (+++) (p-value < 0.05), indicating that the combination treatment of gefitinib and

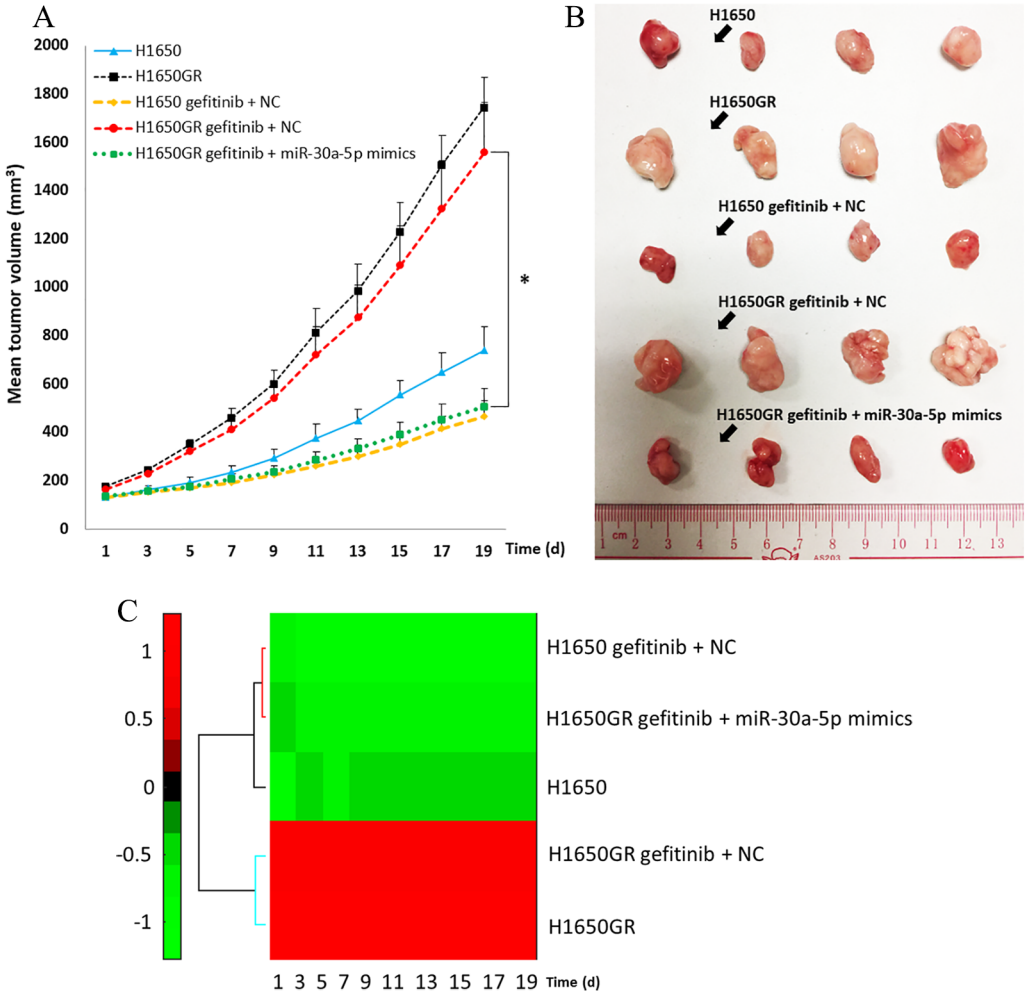

Figure 6. Tumor growth in xenograft mouse models among the H1650, H1650GR, H1650 gefitinib+NC, H1650GR gefitinib+NC, and H1650GR gefitinib+miR-30a-5p groups. (A) Comparison of mean tumor volume from the first to the last day of the observation period. *p-value < 0.05, one-way ANOVA followed by Tukey's *post hoc* test. (B) Tumor samples collected from the five groups after the 3-week treatment. (C) Hierarchical clustering of the mean tumor volume from the five groups.
ANOVA, analysis of variance; NC, negative control.

miR-30a-5p could inhibit the PI3K/AKT signaling pathway *in vivo* (Figure 7).

Discussion

This study explored the effects of a combination therapy of gefitinib and miR-30a-5p in overcoming acquired resistance to EGFR-TKIs through regulating the IGF1R and MET signaling pathways *in vitro* and *in vivo*. The TKRs IGF1R and MET share downstream effector molecules with EGFR. First, drug resistance mechanisms were examined in one gefitinib-sensitive (H1650) and three gefitinib-resistant (H1650GR, H1975, and H460) cell lines. Interestingly, our findings showed that, with increasing concentrations of gefitinib, the IGF1R signaling pathway was activated in the H1650GR, H1975, and H460 cell lines, while the MET signaling pathway was activated only in the H460 cell line (Table S1). Given the different pathways activated in different cell lines, the combination treatment of gefitinib and miR-30a-5p mimics could block downstream signal transduction in H1650GR cell line, and effectively suppress tumor growth in a mouse model induced by the H1650GR cell line, further overcoming drug resistance.

In the gefitinib-sensitive cell line H1650, gefitinib could effectively block the EGFR downstream signaling pathways, since the expression levels of

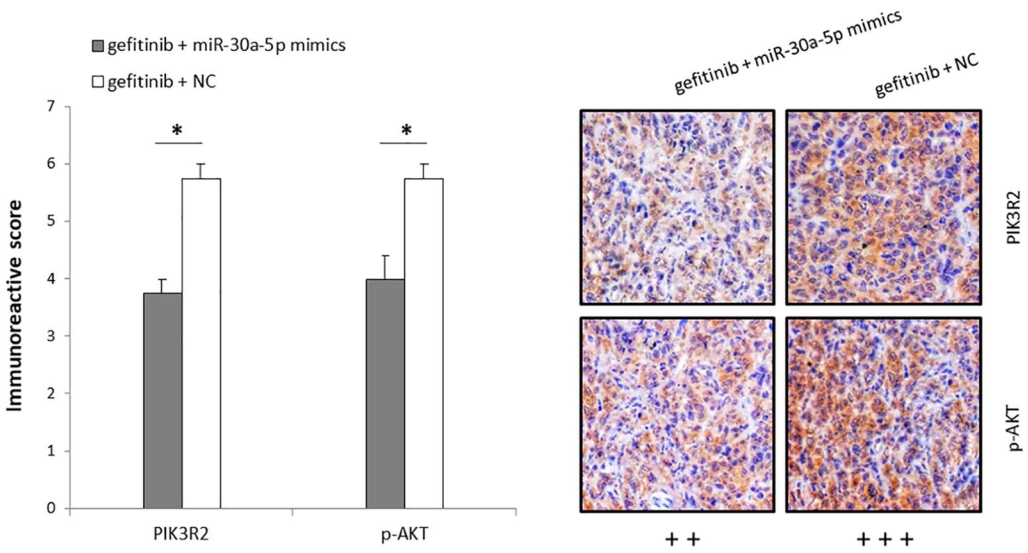

Figure 7. Immunohistochemistry analysis of xenograft tumors after 3-week treatments with gefitinib+miR-30a-5p and gefitinib only, showing expression of PIK3R2 and p-AKT in the H1650GR gefitinib+miR-30a-5p and H1650GR gefitinib+NC groups. The bar chart presents the mean immunoreactive score of PIK3R2 and p-AKT in tumors among four mice.
*p-value < 0.05 in t-test. Representative immunohistochemistry images are shown on the right.

p-EGFR and the downstream molecules p-AKT and p-ERK decreased with increasing concentrations of gefitinib (Figure 1A). After the H1650 cell line was induced to become the H1650GR cell line, gefitinib could inhibit phosphorylation of EGFR, but could not block downstream signal transduction. We showed that the IGF1R pathway was activated in the H1650GR cell line (Figure 1B). It has been reported that redundant signaling through IGF1R could maintain activation of vital pathways for survival when EGFR is inhibited.[33] To our knowledge, there are at least three possible causes leading to gefitinib resistance in NSCLC, which has been summarized in Table S1. Firstly, the T790M mutation of EGFR has been demonstrated in many studies. The T790M mutation increases the recruitment and binding of ATP, to further phosphorylate EGFR to transduce the signals even in the presence of gefitinib.[34,35] Secondly, other TKR signaling pathways sharing the same downstream molecules with EGFR are activated, such as IGF1R and c-MET, which also has been proved in our study (Table S1).[12] A third factor is the gene mutations found in key downstream molecules of the EGFR signaling pathway, such as the G118D mutation in PI3K and Q61H in K-ras.[36] The G118D mutation could lead to increased affinity between PIK3R2 (P85) and PIK3CA (P110), allowing PI3K to gain the ability to activate downstream molecules independent of EGFR activation.[37]

Inhibiting both EGFR and IGF1R could block signal transduction in the PI3K/AKT signaling pathway. AKT is the molecule downstream of PI3K, and expression of its phosphorylated form was lowest in the dual inhibitors group compared with the gefitinib-only and AEW541-only treatment groups (Figure 2). Due to EGFR and IGF1R cross talk, these two pathways could mediate common downstream MAPK and AKT signaling.[38] Clinical data from a cohort of lung cancer patients have proved that EGFR and IGF1R are significantly co-expressed, and a high co-expression level is associated with poor prognosis.[39] Dual inhibition of EGFR and IGF1R has been found to significantly decrease cell growth and invasiveness.[33] Activation of the IGF1R pathway could confer resistance to EGFR inhibitors in EGFR-dependent glioblastoma by regulating AKT, indicating that a concurrent blockade of both EGFR and IGF1R pathways may provide hopeful promise in the treatment of EGFR-dependent glioblastoma.[40] Activation of the IGF1R signaling pathway makes a contribution to afatinib resistance in NSCLC cells with the T790M mutation.[41] Knockdown of IGF1R could overcome resistance to afatinib, and induce apoptosis in afatinib-resistant cells.[41] Dual inhibition of EGFR and other TKRs may not overcome acquired drug resistance, due to the mutation existing in common downstream molecules, including the G118D mutation in PI3K mentioned above. Therefore, it is particularly important to suppress the

common key downstream molecules among different TKR signaling pathways.

The PI3K/AKT pathway is one such vital signaling pathway shared by different TKRs that can lead to cell proliferation and survival.[42,43] It has been confirmed that PI3K inihibtion could restore the gefitinib resistance in xenograft models.[44] In our previous study, we found that knockdown of PI3K had the same effect with the dual inhibition of EGFR and IGF1R to block the signal transduction.[18] In this study, we found that miR-30a-5p could bind to the target genes PIK3R2 and PIK3CD, two subunits of PI3K, and further downregulate the expression levels. Furthermore, treatment with miR-30a-5p mimics induced cell apoptosis, and inhibited cell invasion and migration in the H1650GR cell line (Figure 4). The combination treatment of gefitinib and miR-30a-5p mimics lowered expression levels of p-AKT and p-ERK in the H1650GR cell line, effectively suppressed tumor growth, and further inhibited signal transduction of the PI3K/AKT signaling pathway in xenograft tumor *in vivo* (Figures 5–7). MiRNAs play essential roles in the malignant phenotypes of cancers as these small molecules modulate the aberrant functions of their target genes, including metastasis, multi-drug resistance, proliferation, and the self-renewal or differentiation of cancer stem cells.[45] Other studies have shown that miRNAs are involved in the pathogenesis, diagnosis, and prognosis of lung cancer.[46] MiR-30a could inhibit proliferation and metastasis in many tumors, as well as autophagy in chronic myelogenous leukemia.[47] miR-19a and miR-19b are upregulated in multi-drug resistant cell lines, modulating multi-drug resistance in gastric cancer cells by regulating phosphatase and tensin homolog (PTEN).[48] MiR-153 upregulation could increase the cell invasiveness and resistance to oxaliplatin and cisplatin in colorectal cancer induced by FOXO3a.[49] The miR-134/487b/655 cluster was found to regulate the TGF-β1-induced epithelial-mesenchymal transition (EMT) phenomenon and affect resistance to gefitinib by directly targeting MAGI2 in lung cancer cells.[50] Another study found that the gefitinib-induced apoptosis and EMT of NSCLC cells were affected by miR-30b, miR-30c, miR-221, and miR-222 through inhibiting expression of some important oncogenes.[25] MiRNAs, as anti-oncomiRs, could reverse EGFR-TKI resistance in NSCLC by relevant targets, including EGFR, PI3K, and IGF1R.[51] Thus, miRNAs are poised to become remarkable agents of novel drug discovery in cancer treatment, especially when used together with other agents.[52] Researchers have tested a liposomal nanoparticle loaded with synthetic miRNA-34a mimics (MRX34) combined with the EGFR-TKI, erlotinib, as a promising cancer therapy method.[53,54]

This study used a xenograft model for creating tumor microenvironments with physiological and pathological conditions similar to those of patients. However, the cell lines used cannot reflect the original behaviors of cancer cells due to their artificial nature and adaptations to *in vitro* culture growth conditions.

In this study, we showed that dual inhibition of EGFR and IGF1R could block signal transduction in the PI3K/AKT signaling pathway. The direct inhibition of the shared downstream molecule PI3K was further investigated to improve acquired drug resistance. The combination treatment of gefitinib and miR-30a-5p mimics inhibited signal transduction in the H1650GR cell line, and effectively suppressed tumor growth in the H1650GR xenograft. Hence, the combination therapy of gefitinib and miR-30a-5p may play a critical role in overcoming acquired resistance to EGFR-TKIs, giving new insights into improving cancer treatment.

Author Contribution(s)

Fengfeng Wang: Conceptualization; Data curation; Formal analysis; Methodology; Writing-original draft.

Fei Meng: Conceptualization; Data curation; Formal analysis; Investigation; Methodology; Validation; Writing-original draft.

Sze Chuen Cesar Wong: Conceptualization; Investigation; Methodology; Resources; Validation; Writing-review & editing.

William C.S. Cho: Conceptualization; Methodology; Resources; Validation; Writing-review & editing.

Sijun Yang: Conceptualization; Methodology; Validation; Writing-review & editing.

Lawrence W.C. Chan: Conceptualization; Data curation; Formal analysis; Investigation; Methodology; Project administration; Resources; Supervision; Validation; Writing-original draft; Writing-review & editing.

Funding

The authors disclosed receipt of the following financial support for the research, authorship, and/or publication of this article: This project was supported by two Health and Medical Research Funds (HMRF 02131026 and HMRF 16172561).

Conflict of interest statement

The authors declare that there is no conflict of interest.

Animal welfare

The present study followed international, national and/or institutional guidelines for humane animal treatment and complied with relevant legislation.

ORCID iD

Lawrence W.C. Chan https://orcid.org/0000-0001-6451-2273

Supplemental material

The reviews of this paper are available via the supplemental material section.

References

1. Al-Saleh K, Quinton C and Ellis PM. Role of pemetrexed in advanced non-small-cell lung cancer: meta-analysis of randomized controlled trials, with histology subgroup analysis. *Curr Oncol* 2012; 19: e9.
2. Tang Y-A, Chen C-H, Sun HS, *et al.* Global oct4 target gene analysis reveals novel downstream pten and TNC genes required for drug-resistance and metastasis in lung cancer. *Nucleic Acids Res* 2015; 43: 1593–1608.
3. Indovina P, Marcelli E, Maranta P, *et al.* Lung cancer proteomics: recent advances in biomarker discovery. *Int J Proteomics* 2011; 2011: 726869.
4. Siegel R, Naishadham D and Jemal A. Cancer statistics, 2013. *CA Cancer J Clin* 2013; 63: 11–30.
5. Keith RL and Miller YE. Lung cancer chemoprevention: current status and future prospects. *Nat Rev Clin Oncol* 2013; 10: 334.
6. Liang W, Cai K, Chen C, *et al.* Society for translational medicine consensus on postoperative management of EGFR-mutant lung cancer (2019 edition). *Transl Lung Cancer Res* 2019; 8: 1163–1173.
7. Lynch TJ, Bell DW, Sordella R, *et al.* Activating mutations in the epidermal growth factor receptor underlying responsiveness of non–small-cell lung cancer to gefitinib. *N Engl J Med* 2004; 350: 2129–2139.
8. Shi Y, Au JS-K, Thongprasert S, *et al.* A prospective, molecular epidemiology study of EGFR mutations in asian patients with advanced non–small-cell lung cancer of adenocarcinoma histology (pioneer). *J Thorac Oncol* 2014; 9: 154–162.
9. Sin T, Wang F, Meng F, *et al.* Implications of microRNAs in the treatment of gefitinib-resistant non-small cell lung cancer. *Int J Mol Sci* 2016; 17: 237.
10. Hung L-Y, Tseng JT, Lee Y-C, *et al.* Nuclear epidermal growth factor receptor (EGFR) interacts with signal transducer and activator of transcription 5 (STAT5) in activating Aurora-A gene expression. *Nucleic Acids Res* 2008; 36: 4337–4351.
11. Wang F, Chan LW, Law HK, *et al.* Exploring microRNA-mediated alteration of EGFR signaling pathway in non-small cell lung cancer using an mRNA: miRNA regression model supported by target prediction databases. *Genomics* 2014; 104: 504–511.
12. Camp ER, Summy J, Bauer TW, *et al.* Molecular mechanisms of resistance to therapies targeting the epidermal growth factor receptor. *Clin Cancer Res* 2005; 11: 397–405.
13. Suda K, Murakami I, Sakai K, *et al.* Small cell lung cancer transformation and T790M mutation: complimentary roles in acquired resistance to kinase inhibitors in lung cancer. *Sci Rep* 2015; 5: 14447.
14. Ahn MJ, Tsai CM, Shepherd FA, *et al.* Osimertinib in patients with T790M mutation-positive, advanced non–small cell lung cancer: long-term follow-up from a pooled analysis of 2 phase 2 studies. *Cancer* 2019; 125: 892–901.
15. Ettinger DS, Wood DE, Aggarwal C, *et al.* NCCN guidelines insights: non–small cell lung cancer (version 1.2020). *J Natl Compr Canc Netw* 2019; 17: 1464–1472.
16. Zhang Z, Lee JC, Lin L, *et al.* Activation of the AXL kinase causes resistance to EGFR-targeted therapy in lung cancer. *Nat Genet* 2012; 44: 852.
17. Barr Kumarakulasinghe N, Zanwijk NV and Soo RA. Molecular targeted therapy in the treatment of advanced stage non-small cell lung cancer (NSCLC). *Respirology* 2015; 20: 370–378.
18. Meng F, Wang F, Wang L, *et al.* MiR-30a-5p overexpression may overcome EGFR-inhibitor resistance through regulating PI3K/AKT signaling pathway in non-small cell lung cancer cell lines. *Front Genet* 2016; 7: 197.

19. Wang F, Meng F, Wang L, *et al.* Associations of mRNA: microRNA for the shared downstream molecules of EGFR and alternative tyrosine kinase receptors in non-small cell lung cancer. *Front Genet* 2016; 7: 173.

20. Ponzetto C, Bardelli A, Maina F, *et al.* A novel recognition motif for phosphatidylinositol 3-kinase binding mediates its association with the hepatocyte growth factor/scatter factor receptor. *Mol Cell Biol* 1993; 13: 4600–4608.

21. Skouteris GG and Georgakopoulos E. Hepatocyte growth factor-induced proliferation of primary hepatocytes is mediated by activation of phosphatidylinositol 3-kinase. *Biochem Biophys Res Commun* 1996; 218: 229–233.

22. Mehta R, Katta H, Alimirah F, *et al.* Deguelin action involves c-met and EGFR signaling pathways in triple negative breast cancer cells. *PLoS One* 2013; 8: e65113.

23. Kulik G, Klippel A and Weber MJ. Antiapoptotic signalling by the insulin-like growth factor I receptor, phosphatidylinositol 3-kinase, and akt. *Mol Cell Biol* 1997; 17: 1595–1606.

24. Cho WC. MicroRNAs: potential biomarkers for cancer diagnosis, prognosis and targets for therapy. *Int J Biochem Cell Biol* 2010; 42: 1273–1281.

25. Yeo CD, Park KH, Park CK, *et al.* Expression of insulin-like growth factor 1 receptor (IGF-1R) predicts poor responses to epidermal growth factor receptor (EGFR) tyrosine kinase inhibitors in non-small cell lung cancer patients harboring activating egfr mutations. *Lung Cancer* 2015; 87: 311–317.

26. Zhou J, Wang J, Zeng Y, *et al.* Implication of epithelial-mesenchymal transition in IGF1R-induced resistance to EGFR-TKIs in advanced non-small cell lung cancer. *Oncotarget* 2015; 6: 44332.

27. Hou J, Meng F, Chan LW, *et al.* Circulating plasma micrornas as diagnostic markers for NSCLC. *Front Genet* 2016; 7: 193.

28. Cho WC. MicroRNAs as therapeutic targets for lung cancer. *Expert Opin Ther Targets* 2010; 14: 1005–1008.

29. Hu S, Yuan Y, Song Z, *et al.* Expression profiles of micrornas in drug-resistant non-small cell lung cancer cell lines using microrna sequencing. *Cell Physiol Biochem* 2018; 51: 2509–2522.

30. Han X, Liu M, Wang S, *et al.* An integrative analysis of the putative gefitinib-resistance related genes in a lung cancer cell line model system. *Curr Cancer Drug Targets* 2015; 15: 423–434.

31. Davalos V, Moutinho C, Villanueva A, *et al.* Dynamic epigenetic regulation of the microrna-200 family mediates epithelial and mesenchymal transitions in human tumorigenesis. *Oncogene* 2012; 31: 2062–2074.

32. Cong N, Du P, Zhang A, *et al.* Downregulated microRNA-200a promotes EMT and tumor growth through the Wnt/β-catenin pathway by targeting the e-cadherin repressors ZEB1/ZEB2 in gastric adenocarcinoma. *Oncol Rep* 2013; 29: 1579–1587.

33. Chakravarti A, Loeffler JS and Dyson NJ. Insulin-like growth factor receptor i mediates resistance to anti-epidermal growth factor receptor therapy in primary human glioblastoma cells through continued activation of phosphoinositide 3-kinase signaling. *Cancer Res* 2002; 62: 200–207.

34. Engelman JA and Jänne PA. Mechanisms of acquired resistance to epidermal growth factor receptor tyrosine kinase inhibitors in non–small cell lung cancer. *Clin Cancer Res* 2008; 14: 2895–2899.

35. Riely GJ, Pao W, Pham D, *et al.* Clinical course of patients with non–small cell lung cancer and epidermal growth factor receptor exon 19 and exon 21 mutations treated with gefitinib or erlotinib. *Clin Cancer Res* 2006; 12: 839–844.

36. Pao W and Girard N. New driver mutations in non-small-cell lung cancer. *Lancet Oncol* 2011; 12: 175–180.

37. Ikenoue T, Kanai F, Hikiba Y, *et al.* Functional analysis of PIK3CA gene mutations in human colorectal cancer. *Cancer Res* 2005; 65: 4562–4567.

38. Oliveira S, Schiffelers R, Storm G, *et al.* Crosstalk between epidermal growth factor receptor-and insulin-like growth factor-1 receptor signaling: implications for cancer therapy. *Curr Cancer Drug Targets* 2009; 9: 748–760.

39. Gately K, Forde L, Cuffe S, *et al.* High coexpression of both EGFR and IGF1R correlates with poor patient prognosis in resected non–small-cell lung cancer. *Clin Lung Cancer* 2014; 15: 58–66.

40. Ma Y, Tang N, Thompson RC, *et al.* InsR/IGF1R pathway mediates resistance to EGFR inhibitors in glioblastoma. *Clin Cancer Res* 2016; 22: 1767–1776.

41. Lee Y, Wang Y, James M, *et al.* Inhibition of IGF1R signaling abrogates resistance to afatinib (BIBW2992) in EGFR T790M mutant lung cancer cells. *Mol Carcinog* 2016; 55: 991–1001.

42. Gandhi J, Zhang J, Xie Y, *et al.* Alterations in genes of the egfr signaling pathway and their relationship to EGFR tyrosine kinase inhibitor

sensitivity in lung cancer cell lines. *PLoS One* 2009; 4: e4576.

43. Sharma SV, Bell DW, Settleman J, *et al.* Epidermal growth factor receptor mutations in lung cancer. *Nat Rev Cancer* 2007; 7: 169.
44. Donev IS, Wang W, Yamada T, *et al.* Transient PI3K inhibition induces apoptosis and overcomes HGF-mediated resistance to EGFR-TKIS in EGFR mutant lung cancer. *Clin Cancer Res* 2011; 17: 2260–2269.
45. Wu Q, Yang Z, Nie Y, *et al.* Multi-drug resistance in cancer chemotherapeutics: mechanisms and lab approaches. *Cancer Lett* 2014; 347: 159–166.
46. Wu K-L, Tsai Y-M, Lien C-T, *et al.* The roles of microRNA in lung cancer. *Int J Mol Sci* 2019; 20: 1611.
47. Jiang L-H, Zhang H-D and Tang J-H. Mir-30a: a novel biomarker and potential therapeutic target for cancer. *J Oncol* 2018; 2018: 5167829.
48. Wang F, Li T, Zhang B, *et al.* MicroRNA-19a/b regulates multidrug resistance in human gastric cancer cells by targeting PTEN. *Biochem Biophys Res Commun* 2013; 434: 688–694.
49. Zhang L, Pickard K, Jenei V, *et al.* MiR-153 supports colorectal cancer progression via pleiotropic effects that enhance invasion and chemotherapeutic resistance. *Cancer Res* 2013; 73: 6435–6447.
50. Kitamura K, Seike M, Okano T, *et al.* MiR-134/487b/655 cluster regulates TGF-β–induced epithelial–mesenchymal transition and drug resistance to gefitinib by targeting MAGI2 in lung adenocarcinoma cells. *Mol Cancer Ther* 2014; 13: 444–453.
51. Lu J, Zhan Y, Feng J, *et al.* MicroRNAs associated with therapy of non-small cell lung cancer. *Int J Biol Sci* 2018; 14: 390.
52. Mognato M and Celotti L. MicroRNAs used in combination with anti-cancer treatments can enhance therapy efficacy. *Mini Rev Med Chem* 2015; 15: 1052–1062.
53. Bader AG. MiR-34–a microRNA replacement therapy is headed to the clinic. *Front Genet* 2012; 3: 120.
54. Zhao J, Kelnar K and Bader AG. In-depth analysis shows synergy between erlotinib and miR-34a. *PLoS One* 2014; 9: e89105.